THE QCD POMERON IN e^+e^- COLLISIONS *

J. KWIECIŃSKI

Department of Theoretical Physics
H. Niewodniczański Institute of Nuclear Physics
Radzikowskiego 152, 31-342 Cracow, Poland

AND L. MOTYKA

Institute of Physics, Jagellonian University
Reymonta 4, 30-059 Cracow, Poland

(Received April 19, 1999)

The contribution of the QCD pomeron to the processes: $e^+e^- \to e^+e^- J/\psi J/\psi$ and $e^+e^- \to e^+e^-$ hadrons (with tagged electrons) is discussed. We focus on reactions which occur via photon–photon collisions, with virtual photons coming from the Weizsäcker-Wiliams spectrum of the electrons. We stress the importance of the non-leading corrections to the BFKL equation and take into account dominant non-leading effects which come from the requirement that the virtuality of the exchanged gluons along the gluon ladder is controlled by their transverse momentum squared. The $\gamma^*\gamma^*$ cross-sections are found to increase with increasing $\gamma^*\gamma^*$ CM energy W as $(W^2)^{\lambda_P}$ while the cross-section for J/ψ production is found to increase as $(W^2)^{2\lambda_P}$. The parameter λ_P is slowly varying with energy W and takes the values $\lambda_P \sim 0.23$–0.35 depending on the process. We also analyze the contribution of the soft pomeron for the total $\gamma^*\gamma^*$ cross-section. We compare results of our calculations to the recent data from LEP.

PACS numbers: 12.38.–t, 13.60.Hb, 13.60.Le, 13.65.+i

1. Introduction

Two photon reactions are an important part of physics which is being studied in current e^+e^- experiments at LEP1 and LEP2 and which will also be intensively analyzed in future e^+e^- colliders. The available photon-photon energy and photon virtualities continuously increase with the increasing energy of the e^+e^- pair. Therefore the data from LEP1 and LEP2

* Presented by L. Motyka at the Cracow Epiphany Conference on Electron–Positron Colliders, Cracow, Poland, January 5–10, 1999.

and the expected results from the TESLA and NLC provide us with an excellent opportunity to study virtual photon scattering in the diffractive regime. Moreover, with proper experimental cuts, it is possible to study observables dominated by the perturbative QCD contributions. The theoretical description of such processes is based on expectations concerning high energy limit in perturbative QCD which is at present theoretically fairly well understood [1, 2]. The leading high energy behaviour is controlled by the pomeron singularity which corresponds to the sum of ladder diagrams with reggeized gluons along the chain. This sum is described by the Balitzkij, Fadin, Kuraev, Lipatov (BFKL) equation [3].

The perturbative QCD pomeron exchange effects can be observed only in specific conditions and even then not in the unambiguous form. In order to minimize the contribution of the other mechanisms competing with the QCD pomeron and to guarantee the validity of the calculations based on perturbative QCD one has to chose carefully the processes to analyze. The virtualities of the gluons along the ladder should be large enough to assure the applicability of the perturbative expansion. The necessary hard scale may be provided either by coupling of the ladder to scattering particles, that contain a hard scale themselves, or by large momentum transfer carried by the gluons. Moreover, to distinguish the genuine BFKL from DGLAP evolution effects it is convenient to focus on processes in which the scales on both ends of the ladder are of comparable size. Finally, one requires that the non-perturbative effects should factor out in order to minimize the theoretical uncertainties.

The two classical processes which can probe the QCD pomeron in ep and in $\gamma^* p$ collisions are the deep inelastic events accompanied by an energetic (forward) jet [4, 5] and the production of large p_{T} jets separated by the rapidity gap [6]. The former process probes the QCD pomeron in the forward direction while the latter reflects the elastic scattering of partons via the QCD pomeron exchange with non-zero (and large) momentum transfer. Another possible probe of the QCD pomeron at (large) momentum transfers can be provided by the diffractive vector meson photoproduction accompanied by proton dissociation in order to avoid nucleon form-factor effects [7, 8].

In this talk we shall analyze two measurements in e^+e^- collisions, complementary to those listed above. Namely we focus on double diffractive J/ψ production in $\gamma\gamma$ collisions and on the total $\gamma^*\gamma^*$ cross section. The former process is unique since in principle it allows to test the QCD pomeron for arbitrary momentum transfers [9]. The hard scale is given by the relatively large mass of the c-quark. The total $\gamma^*\gamma^*$ cross-section has been studied by several authors [10, 11], however our approach has the novel feature of taking into account dominant non-leading corrections to the BFKL equation.

This re-analysis has become necessary when the next-to-leading corrections to the BFKL kernel were obtained [12], which alter substantially the results obtained at the leading order. It turns out that the magnitude of the next-to-leading (NLO), *i.e.* $O(\alpha_s^2)$, contribution to the QCD pomeron intercept is very large for the values of the QCD coupling within the range which is relevant for most experiments. This means that the NLO approximation alone is not reliable and one has to perform resummation to all orders. Unfortunately the exact result of this resummation is unknown. It may however be possible to pin down certain dominant contributions of well defined physical origin and perform their exact resummation [13, 14]. In our approach we shall use the so called consistency constraint which limits the available phase space for the real gluon emission by imposing the requirement that the virtuality of the exchanged gluons along the chain is dominated by their transverse momentum squared. Let us remind that the form of the LO BFKL kernel where the gluon propagators contain only the gluon transverse momentum squared etc. is only valid within the region of phase space restricted by this constraint. Formally however, the consistency constraint generates subleading corrections. It can be shown that at the NLO accuracy it generates about 70 % of the exact result for the QCD pomeron intercept. The very important merit of this constraint is also the fact that it automatically generates resummation of higher order contributions which stabilizes the solution [14].

2. The total $\gamma^*\gamma^*$ cross-section

The collisions of virtual photons may be studied experimentally only as subprocesses of reactions between charged particles. In principle, one is able to unfold the photonic cross-section from the leptonic data, however this procedure requires additional assumptions which increase the systematic uncertainty of the result. It seems to be more sensible to formulate the predictions for the e^+e^- cross-sections with the properly chosen cuts and compare them directly with the e^+e^- data. Therefore we use the equivalent photon approximation which allows us to express the leptonic cross-section through a convolution of the photonic cross-section and the standard flux factors. Thus the cross-section for the process $e^+e^- \to e^+e^- + X$ (averaged over the angle ϕ between the lepton scattering planes in the frame in which the virtual photons are aligned along the z axis) is given by the following formula [11]:

$$\frac{Q_1^2 Q_2^2 d\sigma}{dy_1 dy_2 dQ_1^2 dQ_2^2} = \left(\frac{\alpha}{2\pi}\right)^2 \Big[P^{(\mathrm{T})}_{\gamma/e^+}(y_1) P^{(\mathrm{T})}_{\gamma/e^-}(y_2) \sigma^{\mathrm{TT}}_{\gamma^*\gamma^*}(Q_1^2, Q_2^2, W^2) + P^{(\mathrm{T})}_{\gamma/e^+}(y_1) P^{(\mathrm{L})}_{\gamma/e^-}(y_2) \sigma^{\mathrm{TL}}_{\gamma^*\gamma^*}(Q_1^2, Q_2^2, W^2) + P^{(\mathrm{L})}_{\gamma/e^+}(y_1) P^{(\mathrm{T})}_{\gamma/e^-}(y_2) \sigma^{\mathrm{LT}}_{\gamma^*\gamma^*}(Q_1^2, Q_2^2, W^2) + P^{(\mathrm{L})}_{\gamma/e^+}(y_1) P^{(\mathrm{L})}_{\gamma/e^-}(y_2) \sigma^{\mathrm{LL}}_{\gamma^*\gamma^*}(Q_1^2, Q_2^2, W^2) \Big], \quad (1)$$

where

$$P^{(\mathrm{T})}_{\gamma/e}(y) = \frac{1+(1-y)^2}{y}, \quad (2)$$

$$P^{(\mathrm{L})}_{\gamma/e}(y) = 2\frac{1-y}{y}, \quad (3)$$

where y_1 and y_2 are the longitudinal momentum fractions of the parent leptons carried by virtual photons, $Q_i^2 = -q_i^2$ $(i = 1, 2)$ where $q_{1,2}$ denote the four momenta of the virtual photons and W^2 is the total CM energy squared of the two (virtual) photon system, *i.e.* $W^2 = (q_1 + q_2)^2$. The cross-sections $\sigma^{ij}_{\gamma^*\gamma^*}(Q_1^2, Q_2^2, W^2)$ are the total cross-sections for the process $\gamma^*\gamma^* \to X$ and the indices i, j =T,L denote the polarization of the virtual photons. The functions $P^{(\mathrm{T})}_{\gamma/e}(y)$ and $P^{(\mathrm{L})}_{\gamma/e}(y)$ are the transverse and longitudinal photon flux factors.

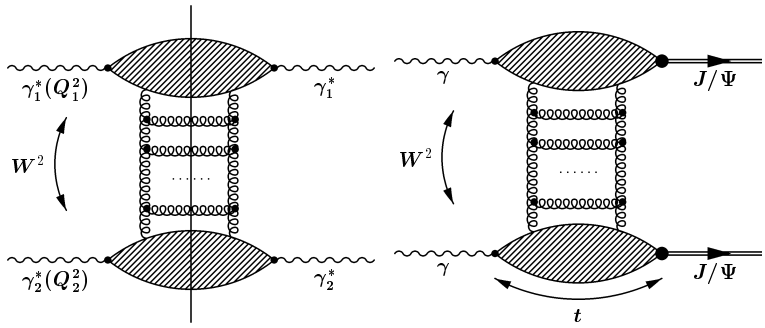

(a) (b)

Fig. 1. The QCD pomeron exchange mechanism of the processes (a) — $\gamma_1^*(Q_1^2)\gamma_2^*(Q_2^2) \to X$ and (b) — $\gamma\gamma \to J/\psi J/\psi$.

The ladder diagram corresponding to the perturbative contribution to the diffractive subprocess $\gamma_1^*(Q_1^2)\gamma^*(Q_2^2) \to X$ is shown in Fig. 1(a). The

cross-sections $\sigma^{ij}_{\gamma^*\gamma^*}(Q_1^2, Q_2^2, W^2)$ are given by the following formulae:

$$\sigma^{ij}_{\gamma^*\gamma^*}(Q_1^2, Q_2^2, W^2) = P_{\rm S}(Q_1^2, Q_2^2, W^2)\delta_{i\rm T}\delta_{j\rm T} + \frac{1}{2\pi}\sum_q \int_{k_0^2}^{k^2_{\max}(Q_2^2,x)} \frac{d^2k}{\pi k^4} \int_{\xi_{\min}(k^2,Q_2^2)}^{1/x} d\xi\, G_q^{0j}(k^2, Q_2^2, \xi)\Phi_i(k^2, Q_1^2, x\xi)\,, \quad (4)$$

where

$$k^2_{\max}(Q_2^2, x) = -4m_q^2 + Q_2^2\left(\frac{1}{x} - 1\right), \quad (5)$$

$$\xi_{\min}(k^2, Q^2) = 1 + \frac{k^2 + 4m_q^2}{Q^2} \quad (6)$$

and

$$x = \frac{Q_2^2}{2q_1q_2}\,. \quad (7)$$

In Eq. (4) we sum over four quark flavours with $m_q \to 0$ for light quarks and $m_c = 1.5$ GeV. The lower limit of integration over k^2 appearing in Eq. (4) is taken to be $k_0^2 = 1$ GeV^2 in order to subtract the contribution from the nonperturbative region from the perturbative part of the amplitude. The functions $G_q^{0i}(k^2, Q^2, \xi)$ are defined as below: [11, 15]

$$G_q^{0T}(k^2, Q^2, \xi) = 2\alpha_{em}\alpha_s(k^2 + m_q^2)e_q^2 \times \int_0^{\lambda_{\max}} d\lambda \int \frac{d^2p'}{\pi}\,\delta\left[\xi - \left(1 + \frac{p'^2 + m_q^2}{z(1-z)Q^2} + \frac{k^2}{Q^2}\right)\right] \times \left\{\left[(z^2 + (1-z)^2)\left(\frac{\boldsymbol{p}}{D_1} - \frac{\boldsymbol{p}+\boldsymbol{k}}{D_2}\right)^2\right] + m_q^2\left(\frac{1}{D_1} - \frac{1}{D_2}\right)^2\right\}, \quad (8)$$

$$G_q^{0L}(k^2, Q^2, \xi) = 8\alpha_{em}\alpha_s(k^2 + m_q^2)e_q^2 \times \int_0^{\lambda_{\max}} d\lambda \int \frac{d^2p'}{\pi}\,\delta\left[\xi - \left(1 + \frac{p'^2 + m_q^2}{z(1-z)Q^2} + \frac{k^2}{Q^2}\right)\right] \times \left[z^2(1-z)^2\left(\frac{1}{D_1} - \frac{1}{D_2}\right)^2\right], \quad (9)$$

where

$$z = \frac{1+\lambda}{2}, \tag{10}$$

$$\boldsymbol{p} = \boldsymbol{p}' + (z-1)\boldsymbol{k}, \tag{11}$$

$$D_1 = p^2 + z(1-z)Q^2 + m_q^2,$$

$$D_2 = (p+k)^2 + z(1-z)Q^2 + m_q^2. \tag{12}$$

In the formulae given above as well as throughout the rest of the text we are using the one loop approximation for the QCD coupling α_s with the number of flavours $N_f = 4$ and set $\Lambda_{\rm QCD} = 0.23$ GeV. The function $P_{\rm S}(Q_1^2, Q_2^2, W^2)$ corresponds to the contribution from the region $k^2 \leq k_0^2$ in the corresponding integrals over the gluon transverse momenta. It is assumed to be dominated by the soft pomeron contribution which is estimated from the factorisation of its couplings, *i.e.*

$$P_S(Q_1^2, Q_2^2, W^2) = \frac{\sigma^{\rm SP}_{\gamma^*(Q_1^2)p}(Q_1^2, W^2)\sigma^{\rm SP}_{\gamma^*(Q_2^2)p}(Q_2^2, W^2)}{\sigma^{\rm SP}_{pp}}. \tag{13}$$

We assume that this term is only contributing to the transverse part. In equation (13) the cross-sections $\sigma^{\rm SP}_{\gamma^*(Q_i^2)p}(Q_i^2, W^2)$ and $\sigma^{\rm SP}_{pp}$ are the soft pomeron contributions to the $\gamma^* p$ and pp total cross sections and their parametrisation is taken from Refs [16, 17]. Their W^2 dependence is, of course, universal *i.e.*

$$\sigma^{\rm SP}_{pp} = \beta_p^2 \left(\frac{W^2}{W_0^2}\right)^{\alpha_{\rm SP}(0)-1},$$

$$\sigma^{\rm SP}_{\gamma^*(Q_i^2)p}(Q_i^2, W^2) = \beta_{\gamma^*}(Q^2)\beta_p \left(\frac{W^2}{W_0^2}\right)^{\alpha_{\rm SP}(0)-1} \tag{14}$$

with $W_0 = 1$ GeV and $\alpha_{\rm SP}(0) \approx 1.08$. The function $\Phi_{\rm T}(k^2, Q^2, x_g)$ satisfies the Balitzkij, Fadin, Kuraev, Lipatov (BFKL) equation which, in the leading $\ln(1/x)$ approximation has the following form:

$$\Phi_i(k^2, Q^2, x_g) = \Phi_i^0(k^2, Q^2, x_g)$$
$$+\Phi^{\rm S}(k^2, Q^2, x_g)\delta_{iT} + \frac{3\alpha_s(k^2)}{\pi}k^2 \int_{x_g}^1 \frac{dx'}{x'} \int_{k_0^2}^\infty \frac{dk'^2}{k'^2}$$
$$\times \left[\frac{\Phi_i(k'^2, Q^2, x') - \Phi_i(k^2, Q^2, x')}{|k'^2 - k^2|} + \frac{\Phi_i(k^2, Q^2, x')}{\sqrt{4k'^4 + k^4}}\right]. \tag{15}$$

In what follows we shall consider the modified BFKL equation in which we restrict the available phase-space in the real gluon emission by the consistency constraint:

$$k'^2 \leq k^2 \frac{x'}{x_g}\,. \tag{16}$$

This constraint follows from the requirement that the virtuality of the exchanged gluons is dominated by their transverse momentum squared. The consistency constraint (16) introduces the non-leading $\ln(1/x)$ effects and in the next-to-leading approximation exhausts about 70% of the entire next-to-leading corrections to the QCD pomeron intercept. The modified BFKL equation takes the following form:

$$\begin{aligned}
&\Phi_i(k^2,Q^2,x_g) = \Phi_i^0(k^2,Q^2,x_g) \\
&+\Phi^S(k^2,Q^2,x_g)\delta_{iT} + \frac{3\alpha_s(k^2)}{\pi}k^2\int\limits_{x_g}^1\frac{dx'}{x'}\int\limits_{k_0^2}^\infty\frac{dk'^2}{k'^2} \\
&\times\left[\frac{\Phi_i(k'^2,Q^2,x')\Theta\left(k^2\frac{x'}{x_g}-k'^2\right)-\Phi_i(k^2,Q^2,x')}{|k'^2-k^2|}+\frac{\Phi_i(k^2,Q^2,x')}{\sqrt{4k'^4+k^4}}\right].
\end{aligned} \tag{17}$$

The inhomogeneous terms in equations (15), (17) are the sum of two contributions $\Phi_i^0(k^2,Q^2,x_g)$ and $\Phi^S(k^2,Q^2,x_g)\delta_{i\mathrm{T}}$. The first term $\Phi_i^0(k^2,Q^2,x_g)$ corresponds to the diagram in which the two gluon system couples to a virtual photon through a quark box and are given by following equations:

$$\Phi_i^0(k^2,Q^2,x_g) = \sum_q\int\limits_{x_g}^1 dz\;\tilde{G}_{iq}^0(k^2,Q^2,z)\,, \tag{18}$$

where

$$\begin{aligned}
&\tilde{G}_{Tq}^0(k^2,Q^2,z) = 2\alpha_{em}e_q^2\alpha_s(k^2+m_q^2) \\
&\times\int\limits_0^1 d\lambda\left\{\frac{[\lambda^2+(1-\lambda)^2][z^2+(1-z)^2]}{\lambda(1-\lambda)k^2+z(1-z)Q^2+m_q^2}\,k^2\right. \\
&\left.+2m_q^2\left[\frac{1}{z(1-z)Q^2+m_q^2}-\frac{1}{\lambda(1-\lambda)k^2+z(1-z)Q^2+m_q^2}\right]\right\},
\end{aligned} \tag{19}$$

$$\tilde{G}^0_{Lq}(k^2,Q^2,z) = 16\alpha_{em}Q^2k^2e_q^2\alpha_s(k^2+m_q^2)$$
$$\times \int_0^1 d\lambda \left\{ \frac{[\lambda(1-\lambda)][z^2(1-z)^2]}{[\lambda(1-\lambda)k^2+z(1-z)Q^2+m_q^2][z(1-z)Q^2+m_q^2]} \right\}. \quad (20)$$

The second term $\Phi^S(k^2,Q^2,x_g)\delta_{i\mathrm{T}}$, which is assumed to contribute only to the transverse component, corresponds to the contribution to the BFKL equation from the nonperturbative soft region $k'^2 < k_0^2$. Adopting the strong ordering approximation $k'^2 \ll k^2$ it is given by the following formula:

$$\Phi^S(k^2,Q^2,x_g) = \frac{3\alpha_s(k^2)}{\pi} \int_{x_g}^1 \frac{dx'}{x'} \int_0^{k_0^2} \frac{dk'^2}{k'^2} \Phi_T(k'^2,Q^2,x'). \quad (21)$$

The last integral in equation (21) can be interpreted as a gluon distribution in a virtual photon of virtuality Q^2 evaluated at the scale k_0^2. At low values of x' it is assumed to be dominated by a soft pomeron contribution and can be estimated using the factorisation of the soft pomeron couplings:

$$\int_0^{k_0^2} \frac{dk'^2}{k'^2} \Phi_T(k'^2,Q^2,x') = \pi^2 x' g_p(x',k_0^2) \frac{\beta_{\gamma^*}(Q^2)}{\beta_p}, \quad (22)$$

where $g_p(x',k_0^2)$ is the gluon distribution in a proton at the scale k_0^2 and the couplings $\beta_{\gamma^*}(Q^2)$ and β_p are defined by equation (14). We adopt the parametrization of the gluon structure function taken from Ref. [15] *i.e.* $xg(x,k_0^2) = 1.57(1-x)^{2.5}$ which is consistent with the DIS data.

In Fig. 2 we show our results for $\sigma^{\mathrm{TT}}_{\gamma^*\gamma^*}(Q_1^2,Q_2^2,W^2)$ plotted as the function of the CM energy W for three different values of Q^2 where $Q_1^2 = Q_2^2 = Q^2$. We plot in this figure:

1. the pure QCD (*i.e.* "hard") contribution obtained from solving the BFKL equation with the consistency constraint included (see Eq. (17)) and with the inhomogeneous term containing only the QCD impact factor defined by equations (18), (19), (20),

2. the "mixed" contribution generated by the BFKL equation (17) with the soft pomeron contribution defined by equations (21), (22) included in the inhomogeneous term,

3. The "full" contribution which also contains the soft pomeron term (13).

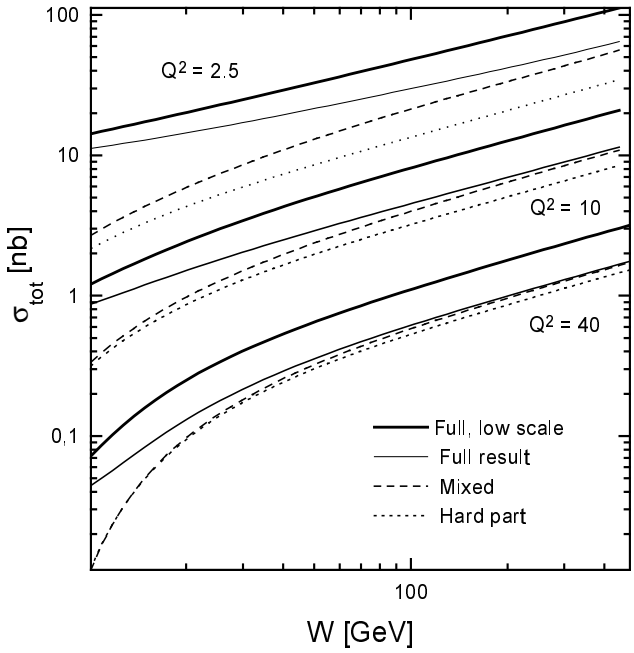

Fig. 2. Energy dependence of the cross-section $\sigma^{\rm TT}_{\gamma^*\gamma^*}(Q_1^2, Q_2^2, W^2)$ for the process $\gamma^*(Q_1^2)\gamma^*(Q_2^2) \to X$ for various choices of virtualities $Q^2 = Q_1^2 = Q_2^2$ corresponding to Eq. (4). For each choice of the virtuality there are shown four curves taking into account hard effects only ("hard part"), hard amplitude with some soft pomeron contributions added ("mixed"), the full cross-section including both soft and hard pomeron contributions ("full result"). We also show the "full result" with low scale of α_s in the impact factors: $\mu^2 = (k^2 + m_q^2)/4$.

We also show results obtained by changing the scale of the strong coupling α_s in the impact factors from $k^2 + m_q^2$ to $(k^2 + m_q^2)/4$. The scale of α_s in the BFKL equation is the same in the both cases. The components of the cross-section for which at least one of the photons is longitudinally polarized have very similar energy dependence to $\sigma^{\rm TT}_{\gamma^*\gamma^*}(Q_1^2, Q_2^2, W^2)$ and give together about 60% of the transverse–transverse contribution.

We see from this figure that the effects of the soft pomeron contribution are non-negligible at low and moderately large values of $Q^2 < 10$ GeV^2 and for moderately large values of $W < 100$ GeV. The QCD pomeron however dominates already at $Q^2 = 40$ GeV^2. We also see from this figure that for low energies $W < 40$ GeV the phase-space effects are very important. For $W > 40$ GeV or so one observes that the cross-section exhibits the

TABLE I

Comparison of the theoretical results to L3 data for $e^+e^- \to e^+e^-X$ with $E_{\rm tag} > 30$ GeV, 30 mrad $< \theta_{\rm tag} <$ 66 mrad. We show in the table $d\sigma/dY$ binned in Y obtained from experiment and the results of our calculation which take into account perturbative pomeron only (hard) and both perturbative and soft pomerons (hard + DL) for two different choices of scale of the α_s in impact factors and for e^+e^- CM energy 91 GeV and 183 GeV.

ΔY	$\langle d\sigma/dY\rangle$ [fb]				
	Data — QPM	Theory (BFKL+DL)			
		$\alpha_s[(\boldsymbol{k}^2+m_q^2)/4]$		$\alpha_s(\boldsymbol{k}^2+m_q^2)$	
		Hard	Hard + DL	Hard	Hard + DL
91 GeV					
2–3	$480 \pm 140 \pm 110$	76	206	34	163
3–4	$240 \pm 60 \pm 50$	114	237	53	173
4–6	$110 \pm 30 \pm 10$	60	109	29	74
183 GeV					
2–3	$180 \pm 120 \pm 50$	51	68	25	42
3–4	$160 \pm 50 \pm 30$	70	86	34	49
4–6	$120 \pm 40 \pm 20$	70	85	35	47

effective power-law behaviour $\sigma_{\gamma^*\gamma^*}(W) \sim (W^2)^{\lambda_{\rm P}}$. The (effective) exponent increases weakly with increasing Q^2 and varies from $\lambda_{\rm P} = 0.28$ for $Q^2 = 2.5$ GeV^2 to $\lambda_{\rm P} = 0.33$ for $Q^2 = 40$ GeV^2. This (weak) dependence of the effective exponent $\lambda_{\rm P}$ with Q^2 is the result of the interplay between soft and hard pomeron contributions, where the former becomes less important at large Q^2.

Using Formula (1) integrated over the virtualities in the range allowed by the relevant experimental cuts, we have calculated the total cross-section for the process $e^+e^- \to e^+e^- + X$ for LEP1 and LEP2 energies and confronted results of our calculation with the recent experimental data obtained by the L3 collaboration at LEP [18]. Comparison of our results with experimental data is summarized in Table I. We show comparison for $d\sigma/dY$, where $Y = \ln(W^2/Q_1Q_2)$ with subtracted Quark Parton Model (QPM) contribu-

tion. We see that the contamination of the cross-section by soft pomeron is substantial. The data do also favour the smaller value of the scale of α_s. In general, the results of our calculation lay below the data, however the error bars are still quite large, so that the discrepancy is not very pronounced. Let us also mention that cuts applied to obtain the data shown in Table 1 admit rather low $\gamma\gamma$ energies *i.e.* below 10 GeV [18], which probably is not sufficient to justify the validity of high energy limit in QCD.

3. Exclusive J/ψ production

The experimental aspects of the measurement of double exclusive J/ψ production are different from those for the virtual photons scattering. Namely, since the c-quark provides the energy scale, we may perturbatively describe the cross-section for the process of exclusive J/ψ production in which almost real photons take part. It is an important feature because the photon flux in electron is dominated by low virtualities. On the other hand one may measure the produced J/ψ-s through theirs decay products with no need of tagging of the electrons. Thus, it is preferred to focus on events with anti-tagged leptons. The cross-section for the process $e^+e^- \to e^+e^- + Y$ for anti-tagged $e^\pm$ corresponds to the production of the hadronic state Y in $\gamma\gamma$ collision and is given by the following convolution integral: [19]

$$\sigma_{e^+e^-\to e^+e^-+Y} = \int_0^1 dy_1 \int_0^1 dy_2 \Theta(W^2 - W_{Y0}^2) \sigma_{\gamma\gamma\to Y}(W^2) f_{\gamma/e}(y_1) f_{\gamma/e}(y_2)\,, \tag{23}$$

where the $\gamma\gamma$ system invariant mass squared W^2 is related to the lepton CM energy squared s by the simple formula: $W^2 = y_1 y_2 s$. The flux factor takes the form:

$$f_{\gamma/e}(y) = \frac{\alpha_{em}}{2\pi}\left[\frac{1+(1-y)^2}{y}\ln\frac{Q^2_{\max}}{Q^2_{\min}} - 2m_e^2 y\left(\frac{1}{Q^2_{\min}} - \frac{1}{Q^2_{\max}}\right)\right] \tag{24}$$

and

$$Q^2_{\min} = \frac{m_e^2 y^2}{(1-y)}\,, \tag{25}$$

$$Q^2_{\max} = (1-y)E^2_{\rm beam}\theta^2_{\max}\,. \tag{26}$$

The lower limit follows from the kinematics of photon emission from a lepton whereas the upper one arises from the upper limit $\theta_{\max}$ for the lepton scattering angle. The minimal invariant mass squared of the hadronic system W^2_{Y0}, the angle $\theta_{\max}$ and the beam energy $E_{\rm beam}$ depend on the process

and experimental conditions. For diffractive J/ψ production we shall choose $\theta_{\max} = 30$ mrad in accordance with LEP conditions and $W_{Y0} = 15$ GeV.

The formalism that we shall employ to evaluate the cross-section of the sub-process $\gamma\gamma \to J/\psi J/\psi$ is very similar to this used in the previous section. However some modification are necessary in order to adopt to specific features of the process. First of all we have to go beyond the forward configuration of the pomeron by the use of the BFKL equation with non-zero momentum transfer. Besides that, we introduce a parameter s_0 in the propagators of exchanged gluons instead of the infra-red cut-off k_0^2 applied in the previous case. This parameter can be viewed upon as the effective representation of the inverse of the colour confinement radius squared. Sensitivity of the cross-section to its magnitude can serve as an estimate of the sensitivity of the results to the contribution coming from the infrared region. It should be noted that formula (27) gives finite result in the limit $s_0 = 0$. While analyzing this process we use the asymptotic (high-energy) form of the amplitude, neglecting the phase space effects.

The imaginary part $\mathrm{Im}A(W^2, t = -Q_{\mathrm{P}}^2)$ of the amplitude for the considered process which corresponds to the diagram in Fig. 1(b) can be written in the following form:

$$\mathrm{Im}A(W^2, t = -Q_{\mathrm{P}}^2) = \int \frac{d^2\boldsymbol{k}}{\pi} \frac{\Phi_0(k^2, Q_{\mathrm{P}}^2)\Phi(x, \boldsymbol{k}, \boldsymbol{Q}_{\mathrm{P}})}{\left[\left(\boldsymbol{k} + \frac{\boldsymbol{Q}_{\mathrm{P}}}{2}\right)^2 + s_0\right]\left[\left(\boldsymbol{k} - \frac{\boldsymbol{Q}_{\mathrm{P}}}{2}\right)^2 + s_0\right]}. \quad (27)$$

In this equation $x = m_{J/\psi}^2/W^2$ where W denotes the total CM energy of the $\gamma\gamma$ system, $m_{J/\psi}$ is the mass of the J/ψ meson, $\boldsymbol{Q}_{\mathrm{P}}/2 \pm \boldsymbol{k}$ denote the transverse momenta of the exchanged gluons and $\boldsymbol{Q}_{\mathrm{P}}$ is the transverse part of the momentum transfer.

The impact factor $\Phi_0(k^2, Q_{\mathrm{P}}^2)$ describes the $\gamma J/\psi$ transition induced by two gluons and the diagrams defining this factor are illustrated in Fig. 3. In the nonrelativistic approximation they give the following formula for $\Phi_0(k^2, Q_{\mathrm{P}}^2)$ [7,20]:

$$\Phi_0(k^2, Q_{\mathrm{P}}^2) = \frac{C}{2}\sqrt{\alpha_{em}}\alpha_s(\mu^2)\left[\frac{1}{\bar{q}^2} - \frac{1}{\frac{m_{J/\psi}^2}{4} + k^2}\right], \quad (28)$$

where

$$C = q_c \frac{8}{3}\pi m_{J/\psi} f_{J/\psi} \quad (29)$$

with $q_c = 2/3$ denoting the charge of a charm quark and

$$\bar{q}^2 = \frac{m_{J/\psi}^2 + Q_{\mathrm{P}}^2}{4}, \quad (30)$$

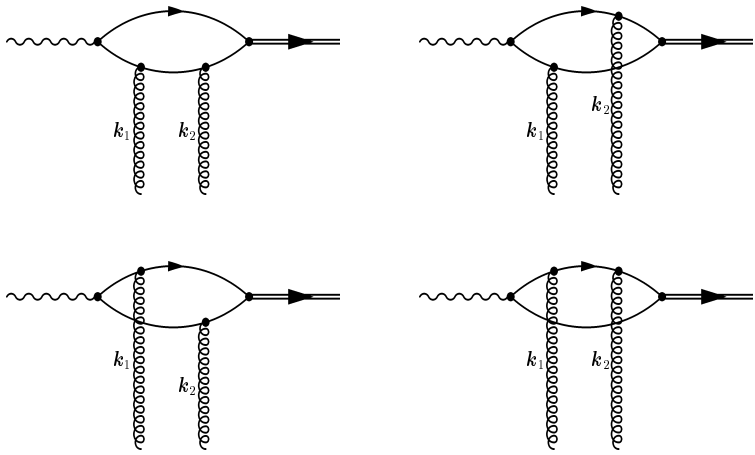

Fig. 3. The diagrams describing the coupling of two gluons to the $\gamma \to J/\psi$ transition vertex.

$$f_{J/\psi} = \sqrt{\frac{3m_{J/\psi}\Gamma_{J/\psi\to l^+l^-}}{2\pi\alpha_{\rm em}^2}}\,, \tag{31}$$

where $\Gamma_{J/\psi\to l^+l^-}$ is the leptonic with of the J/ψ meson. In our calculations we will set $f_{J/\psi} = 0.38$ GeV. The function $\Phi(x, \boldsymbol{k}, \boldsymbol{Q}_{\rm P})$ satisfies the non-forward BFKL equation which in the leading $\ln(1/x)$ approximation has the following form:

$$\Phi(x,\boldsymbol{k},\boldsymbol{Q}_{\rm P}) = \Phi_0(k^2,Q_{\rm P}^2) + \frac{3\alpha_s(\mu^2)}{2\pi^2}\int\limits_x^1 \frac{dx'}{x'}\int \frac{d^2\boldsymbol{k}'}{(\boldsymbol{k}'-\boldsymbol{k})^2+s_0}$$
$$\times\left\{\left[\frac{\boldsymbol{k}_1^2}{\boldsymbol{k}_1'^2+s_0}+\frac{\boldsymbol{k}_2^2}{\boldsymbol{k}_2'^2+s_0}-Q_{\rm P}^2\frac{(\boldsymbol{k}'-\boldsymbol{k})^2+s_0}{(\boldsymbol{k}_1'^2+s_0)(\boldsymbol{k}_2'^2+s_0)}\right]\Phi(x',\boldsymbol{k}',\boldsymbol{Q}_{\rm P})\right.$$
$$\left.-\left[\frac{\boldsymbol{k}_1^2}{\boldsymbol{k}_1'^2+(\boldsymbol{k}'-\boldsymbol{k})^2+2s_0}+\frac{\boldsymbol{k}_2^2}{\boldsymbol{k}_2'^2+(\boldsymbol{k}'-\boldsymbol{k})^2+2s_0}\right]\Phi(x',\boldsymbol{k},\boldsymbol{Q}_{\rm P})\right\}, \tag{32}$$

where

$$\boldsymbol{k}_{1,2} = \frac{\boldsymbol{Q}_{\rm P}}{2} \pm \boldsymbol{k}$$

and

$$\boldsymbol{k}'_{1,2} = \frac{\boldsymbol{Q}_{\rm P}}{2} \pm \boldsymbol{k}' \tag{33}$$

denote the transverse momenta of the gluons. The scale of the QCD coupling α_s which appears in equations (28) and (32) will be set $\mu^2 = k^2 + Q_{\rm P}^2/4 + m_c^2$

where m_c denotes the mass of the charmed quark. The differential cross-section is related in the following way to the amplitude A:

$$\frac{d\sigma}{dt} = \frac{1}{16\pi}|A(W^2,t)|^2. \tag{34}$$

Generalization of the consistency constraint (16) to the case of non-forward configuration with $Q_{\rm P}^2 \geq 0$ takes the following form:

$$k'^2 \leq (k^2 + Q_{\rm P}^2/4)\frac{x'}{x}\,. \tag{35}$$

Besides the BFKL equation (32) in the leading logarithmic approximation we shall also consider the equation which will embody the constraint (35) in order to estimate the effect of the non-leading contributions.

The corresponding equation which contains constraint (35) in the real emission term reads:

$$\begin{aligned}\Phi(x,\boldsymbol{k},\boldsymbol{Q}_{\rm P}) &= \Phi_0(k^2,Q_{\rm P}^2) + \frac{3\alpha_s(\mu^2)}{2\pi^2}\int\limits_x^1 \frac{dx'}{x'}\int \frac{d^2\boldsymbol{k}'}{(\boldsymbol{k}'-\boldsymbol{k})^2+s_0}\\
&\times\left\{\left[\frac{\boldsymbol{k}_1^2}{\boldsymbol{k}_1'^2+s_0}+\frac{\boldsymbol{k}_2^2}{\boldsymbol{k}_2'^2+s_0}-Q_{\rm P}^2\frac{(\boldsymbol{k}'-\boldsymbol{k})^2+s_0}{(\boldsymbol{k}_1'^2+s_0)(\boldsymbol{k}_2'^2+s_0)}\right]\right.\\
&\times\Theta\left((k^2+Q_{\rm P}^2/4)x'/x-k'^2\right)\Big)\,\Phi(x',\boldsymbol{k}',\boldsymbol{Q}_{\rm P})\\
&-\left.\left[\frac{\boldsymbol{k}_1^2}{\boldsymbol{k}_1'^2+(\boldsymbol{k}'-\boldsymbol{k})^2+2s_0}+\frac{\boldsymbol{k}_2^2}{\boldsymbol{k}_2'^2+(\boldsymbol{k}'-\boldsymbol{k})^2+2s_0}\right]\Phi(x',\boldsymbol{k},\boldsymbol{Q}_{\rm P})\right\}.\end{aligned} \tag{36}$$

We solved equations (32) and (36) numerically setting $m_c = m_{J/\psi}/2$. Brief summary of the numerical method and of the adopted approximations in solving equations (32), (36) has been given in Ref. [9]. Let us recall that we used running coupling with the scale $\mu^2 = k^2 + Q_{\rm P}^2/4 + m_c^2$. The parameter s_0 was varied within the range $0.04\ \text{GeV}^2 < s_0 < 0.16\ \text{GeV}^2$. It should be noted that the solutions of equations (32, 36) and the amplitude (27) are finite in the limit $s_0 = 0$. This follows from the fact that both impact factors $\Phi_0(k^2,Q_{\rm P}^2)$ and $\Phi(x,\boldsymbol{k},\boldsymbol{Q}_{\rm P})$ vanish for $\boldsymbol{k} = \pm\boldsymbol{Q}_{\rm P}/2$ (see equations (28), (32), (36)). The results with finite s_0 are however more realistic.

In Fig. 4 we show the cross-section for the process $\gamma\gamma \to J/\psi J/\psi$ plotted as the function of the total CM energy W. We show results based on the BFKL equation in the leading logarithmic approximation as well as those which include the dominant non-leading effects. The calculations were performed for the two values of the parameter s_0 *i.e.* $s_0 = 0.04\ \text{GeV}^2$ and $s_0 = 0.16\ \text{GeV}^2$. In Fig. 5 we show the t-dependence of the cross-section

calculated for $s_0 = 0.10\ \mathrm{GeV}^2$. We show in this Figure results for two values of the CM energy W ($W = 50$ GeV and $W = 125$ GeV) obtained from the solution of the BFKL equation with the non-leading effects taken into account (see Eq. (36)) and confront them with the Born term which corresponds to the two (elementary) gluon exchange. The latter is of course independent of the energy W. The values of the energy W were chosen to be in the region which may be accessible at LEP2. Let us discuss crucial features of the obtained results:

1. *Non leading corrections.* We see from Fig. 4 that the effect of the non-leading contributions is very important and that they significantly reduce magnitude of the cross-section and slow down its increase with increasing CM energy W.

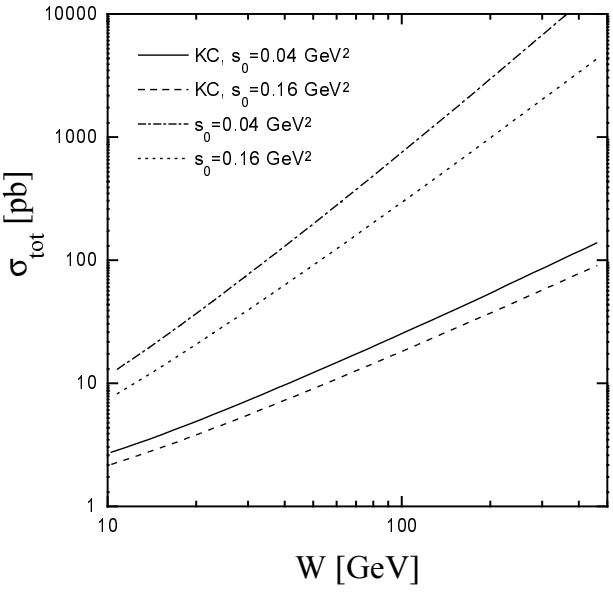

Fig. 4. Energy dependence of the cross-section for the process $\gamma\gamma \to J/\psi J/\psi$. The two lower curves correspond to the calculations based on equation (36) which contains the non-leading effects coming from the constraint (35). The continuous line corresponds to $s_0 = 0.04\ \mathrm{GeV}^2$ and the dashed line to $s_0 = 0.16\ \mathrm{GeV}^2$. The two upper curves correspond to equation (32) *i.e.* to the BFKL equation in the leading logarithmic approximation. The dashed-dotted line corresponds to $s_0 = 0.04\ \mathrm{GeV}^2$ and short dashed line to $s_0 = 0.16\ \mathrm{GeV}^2$.

2. *Energy dependence.* The cross-section exhibits approximate $(W^2)^{2\lambda_P}$ dependence. The parameter λ_P, which slowly varies with the energy W takes the values $\lambda_P \sim 0.23 - 0.28$ within the energy range $20\ \text{GeV} < W < 500\ \text{GeV}$ relevant for LEP2 and for possible TESLA measurements. These results correspond to the solution of the BFKL equation (36) which contains the non-leading effects generated by the constraint (35). The (predicted) energy dependence of the cross-section ($(W^2)^{2\lambda_P}$, $\lambda_P \sim 0.23$–0.28) is marginally steeper than that observed in J/ψ photo-production [21]. It should however be remembered that the non-leading effects which we have taken into account although being the dominant ones still do not exhaust all next-to-leading QCD corrections to the BFKL kernel [12]. The remaining contributions are expected to reduce the parameter λ_P but their effect may be expected to be less important than that generated by the constraint (35). The cross-section calculated from the BFKL equation in the leading logarithmic approximation gives much stronger energy dependence of the cross-section (see Fig. 4).

3. *The value of the cross-section.* Enhancement of the cross-section is still appreciable after including the dominant non-leading contribution which follows from the constraint (35). Thus while in the Born approximation (*i.e.* for the elementary two gluon exchange which gives energy independent cross-section) we get $\sigma_{\text{tot}} \sim 1.9 - 2.6$ pb the cross-section calculated from the solution of the BFKL equation with the non-leading effects taken into account can reach the value 4 pb at $W = 20$ GeV and 26 pb for $W = 100$ GeV *i.e.* for energies which can be accessible at LEP2.

4. *Infrared sensitivity.* The magnitude of the cross-section decreases with increasing magnitude of the parameter s_0 which controls the contribution coming from the infrared region. This effect is however much weaker than that generated by the constraint (35) which gives the dominant non-leading contribution. The energy dependence of the cross-section is practically unaffected by the parameter s_0.

5. *The t-dependence.* Plots shown in Fig. 5 show that the BFKL effects significantly affect the t-dependence of the differential cross-section leading to steeper t-dependence than that generated by the Born term. Possible energy dependence of the diffractive slope is found to be very weak (see Fig. 5). Similar result was also found in the BFKL equation in the leading logarithmic approximation [8].

In our calculations we have assumed dominance of the imaginary part of the production amplitude. The effect of the real part can be taken into ac-

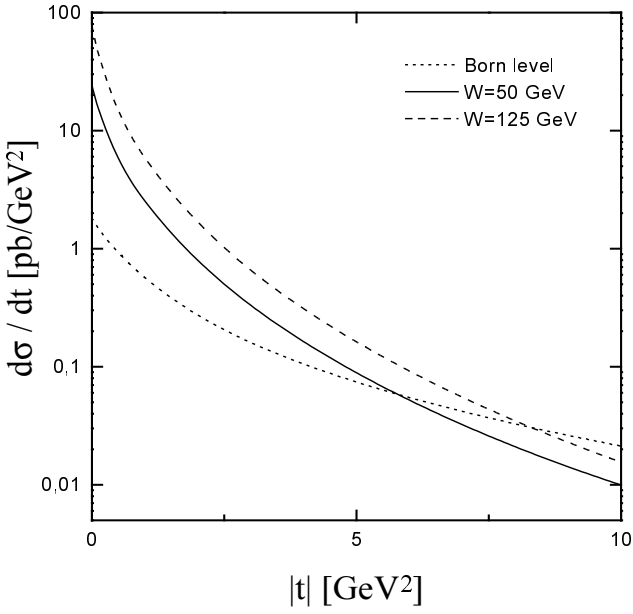

Fig. 5. The differential cross-section of the process $\gamma\gamma \to J/\psi J/\psi$ corresponding to the solution of equation (36) which contains the non-leading effects coming from the consistency (kinematical) constraint (35) shown for two values of the CM energy W, $W = 50\,\mathrm{GeV}$ (continuous line) and $W = 125\,\mathrm{GeV}$ (dashed line). The short dashed line corresponds to the Born term *i.e.* to the elementary two gluon exchange mechanism which gives the energy independent cross-section. The parameter s_0 was set equal to $0.10\,\mathrm{GeV}^2$.

count by multiplying the cross-section by the correction factor $1+tg^2(\pi\lambda_{\mathrm{P}}/2)$ which for $\lambda_{\mathrm{P}} \sim 0.25$ can introduce additional enhancement of about 20 %.

The photonic cross-sections that we obtained in this Section are rather low in terms of the expected number of events, at least for the LEP2 luminosity. Therefore we consider the most inclusive observables relevant for double J/ψ production in e^+e^- collisions which is the total cross-section $\sigma_{\mathrm{tot}}(e^+e^- \to e^+e^- J/\psi J/\psi)$. In fact, it is convenient to impose additionally the anti-tagging condition. Taking $\theta_{\mathrm{max}} = 30$ mrad we get for the $\sigma_{\mathrm{tot}}(e^+e^- \to e^+e^- J/\psi J/\psi)$ the values of about 0.14 pb at $\sqrt{s} = 175$ GeV and 0.74 pb at $\sqrt{s} = 500$ GeV (*i.e.* for typical energies at LEP2 and TESLA respectively). Therefore, assuming the LEP2 luminosity to be about

500 pb^{-1} we predict about 70 events, which is far below the previous expectations [19]. Besides, if one measures both the J/ψ-s through the leptonic decay channels the rate should be divided by factor of about 20, which cuts down the statistics to only a few events.

4. Discussion and summary

From the theoretical point of view, there exist excellent oportunities to study the exchange of the QCD pomeron in e^+e^- colliders. The two golden-plated measurements for this purpose are exclusive J/ψ production and the total $\gamma^*\gamma^*$ cross-section. Both these processes allow to reduce substantially the contribution of unknown, nonperturbative elements. However, the leptonic cross-sections in both cases are well below 1 pb in LEP2 conditions, which makes the measurement rather difficult there. Nevertheless this problem does not appear at the future linear colliders e^+e^- for which the luminosity is expected to be much larger than at LEP and moreover the cross-section for diffractive processes is enhanced due to the photon flux and the pomeron effects. The large expected statistics enables one to reach the region of large photon virtualities (for double tagged events) where the perturbative calculations are more reliable.

The important point that should be stressed once more is the existence of large non-leading corrections to BFKL equation, which influence dramatically the theoretical estimate of the pomeron intercept *i.e.* the behaviour of the cross-sections as functions of the energy. The recently calculated magnitude of next-to-leading contribution to the intercept (for any relevant value of the strong coupling constant) is comparable or even greater than the leading term. This implies a very poor convergence of the perturbative series. Thus one is forced to rely on a resummation scheme. We adopt the so called consistency constraint, which is based on the requirement that the virtualities of gluons exchanged along the ladder are dominated by transverse momenta squared. This constraint introduces at the next-to-leading order a correction to the pomeron intercept which exhausts about 70% of the exact QCD result. The main advantage of this approach is that there is a good physical motivation behind it. Moreover it also offers an approximate resummation scheme for the perturbative expansion of the intercept.

Employing this scheme we found significant reduction of the predicted value of the intercept in comparison to the leading value. We find that the calculated behaviour of the cross-sections exhibit approximate power law dependence $(W^2)^{\lambda_P}$ with $0.28 < \lambda_P < 0.35$ for the total $\gamma^*\gamma^*$ cross-section and $(W^2)^{2\lambda_P}$ with λ_P varying from 0.23 to 0.28 for J/ψ production. This has important consequences for the phenomenology, since the enhancement of the cross-section although still quite appreciable is much smaller than that

which follows from estimates based on the leading logarithmic approximation [19]. The results of our calculation are in fair agreement with the existing data for $\gamma^*\gamma^*$ cross-section from LEP, although the theoretical calculations have a tendency to underestimate experimental results. They are also much more realistic than the predictions following from the leading order BFKL equation, which are an order of magnitude larger. The encouraging element is that even this very first data with rather low statistics, are enough to show clearly the importance of non-leading corrections. We may therefore expect that when the excellent data from linear colliders will be available we will acquire very good opportunity to test our models and to understand more deeply the physics of the QCD pomeron.

We are grateful to the Organizers for the interesting and stimulating Conference. We thank Albert De Roeck for his interest in this work and useful discussions. This research was partially supported by the Polish State Committee for Scientific Research (KBN) grants 2 P03B 184 10, 2 P03B 89 13, 2 P03B 084 14 and by the EU Fourth Framework Programme 'Training and Mobility of Researchers', Network 'Quantum Chromodynamics and the Deep Structure of Elementary Particles', contract FMRX–CT98–0194.

REFERENCES

[1] L.N. Gribov, E.M. Levin, M.G. Ryskin, *Phys. Rep.* **100**, 1 (1983).

[2] L.N. Lipatov, *Phys. Rep.* **286**, 131 (1997).

[3] E.A. Kuraev, L.N.Lipatov, V.S. Fadin, *Zh. Eksp. Teor. Fiz.* **72**, 373 (1977), (Sov. Phys. JETP **45**, 199 (1977)); Ya.Ya. Balitzkij, L.N. Lipatov, *Yad. Fiz.* **28**, 1597 (1978) (*Sov. J. Nucl. Phys.* **28**, 822 (1978)); J.B. Bronzan, R.L. Sugar, *Phys. Rev.* **D17**, 585 (1978); T. Jaroszewicz, *Acta Phys. Pol.* **B11**, 965 (1980); L.N. Lipatov, in "Perturbative QCD", edited by A.H. Mueller, World Scientific, Singapore 1989, p. 441.

[4] A.H. Mueller, *J. Phys. G* **17**, 1443 (1991).

[5] J. Bartels, M. Loewe, A. De Roeck, *Z. Phys.* **C54**, 635 (1992);J. Kwieciński, A.D. Martin, P.J. Sutton, *Phys. Rev.* **D46**, 921 (1992); *Phys. Lett.* **B287**, 254 (1992);J. Bartels *et al.*, *Phys. Lett.* **B384**, 300 (1996); J. Bartels, V. Del Duca, M. Wüsthoff, *Z. Phys.* **C76**, 75 (1997); E. Mroczko, Proceedings of the 28th International Conference on High Energy Physics, Warsaw, Poland, 25–31 July 1996, Z. Ajduk and A.K Wróblewski (editors), World Scientific.

[6] A.H. Mueller, W.K. Tang, *Phys. Lett.* **B284**, 123 (1992); V. Del Duca, W.K. Tang, *Phys. Lett.* **B312**, 225 (1993); V. Del Duca, C.R. Schmidt, *Phys. Rev.* **D49**, 4510 (1994).

[7] J.R. Forshaw, M.G. Ryskin, *Z. Phys.* **C68**, 137 (1995).

[8] J. Bartels, J.R. Forshaw, H. Lotter, M. Wüsthoff, *Phys. Lett.* **B375**, 301 (1996).

[9] J. Kwieciński, L. Motyka, *Phys. Lett.* **B438**, 203 (1998).

[10] J. Bartels, A. De Roeck, H. Lotter, *Phys. Lett.* **B389**, 742 (1996); J. Bartels , A. De Roeck, C. Ewerz, H. Lotter, hep-ph/9710500; A. Białas, W. Czyż, W. Florkowski, *Eur. Phys. J.* **C2**, 683 (1998); W. Florkowski, *Acta Phys. Pol.* **28**, 2673 (1997); A. Donnachie, H.G. Dosch, M. Reuter, *Phys. Rev.* **D59**, 74011 (1999); M. Boonekamp *et al.* hep-ph/9812523.

[11] S.J. Brodsky, F. Hautmann, D.A. Soper, *Phys. Rev.* **D56**, 6957 (1997); *Phys. Rev. Lett.* **78**, 803 (1997) (Erratum, *Phys. Rev. Lett.* **79**, 3544 (1997)).

[12] M. Ciafaloni, G. Camici, *Phys. Lett.* **B386**, 341 (1996); *Phys. Lett.* **B412**, 396 (1997); Erratum, *Phys. Lett.* **B417**, 390 (1998); hep-ph/9803389; M. Ciafaloni, hep-ph/9709390; V.S. Fadin, M.I. Kotskii, R. Fiore, *Phys. Lett.* **B359**, 181 (1995); V.S. Fadin, M.I. Kotskii, L.N. Lipatov, hep-ph/9704267; V.S. Fadin, R. Fiore, A. Flachi, M. Kotskii, *Phys. Lett.* **B422**, 287 (1998); V.S. Fadin, L.N. Lipatov, hep-ph/9802290.

[13] D.A. Ross, *Phys. Lett.* **B431**, 161 (1998); G.P. Salam, JHEP **9807**, 19 (1998); hep-ph/9806482; M. Ciafaloni, D. Colferai hep-ph/9812366; S.J. Brodsky *et al.* hep-ph/9901229.

[14] B. Andersson, G. Gustafson, H. Kharraziha, J. Samuelsson, *Z. Phys.* **C71**, 613 (1996); J. Kwieciński, A.D. Martin, P.J. Sutton, *Z. Phys.* **C71**, 585 (1996).

[15] J. Kwieciński, A.D. Martin, A. Staśto, *Phys. Rev.* **D56**, 3991 (1997).

[16] A. Donnachie, P.V. Landshoff, *Phys. Lett.* **B296**, 227 (1992).

[17] A. Donnachie, P.V. Landshoff, *Z. Phys.* **C61**, 139 (1994).

[18] L3 collaboration, (M. Acciari *et al.*) CERN-EP-98-205 (1998).

[19] Report of the Working Group on "$\gamma\gamma$ physics", P. Aurenche and G. A. Schuler (convenerrs), Proceedings of the Workshop on Physics at LEP2, editors: G. Altarelli, T. Sjöstrand and P. Zwirner, CERN yellow preprint 96-01.

[20] I.F. Ginzburg, S.L. Panfil, V.G. Serbo, *Nucl. Phys.* **B296**, 569 (1988).

[21] S. Aid *et al.*, H1 Collaboration, *Nucl. Phys.* **B468**, 3 (1996); *Nucl. Phys.* **B472**, 3 (1996); M. Derrick *et al.*, ZEUS Collaboration, *Phys. Lett.* **B350**, 120 (1996); J. Breitweg *et al.*, ZEUS Collaboration, *Z. Phys.* **C75**, 215 (1975).